PROCEEDINGS OF SCIENCE

Higgs boson results from the LHC Run-1

Silvio Donato[*†]
Author University of Zurich
E-mail: silvio.donato@cern.ch

The discovery of the Higgs boson has been an important success of the LHC Run 1. This document presents the combination of the ATLAS and CMS measurements of the Higgs boson production and decay rates and of the Higgs boson coupling with vector bosons and fermions. The analysis uses the LHC proton–proton collision data recorded by the ATLAS and CMS experiments in 2011 and 2012, corresponding to integrated luminosities per experiment of approximately 5 fb^{-1} at $\sqrt{s} = 7$ TeV and 20 fb^{-1} at $\sqrt{s} = 8$ TeV. The Higgs boson production and decay rates measured by the two experiments have been combined using different parameterizations. The total Higgs boson cross-section has been measured to be 1.09 ± 0.11 the Standard Model prediction. The combination of the ATLAS and CMS results gives observed significances for the vector boson fusion production process and for the $H \to \tau\tau$ decay of 5.4 and 5.5 standard deviations, respectively. The data are consistent with the Standard Model predictions for all parameterizations considered.

Fourth Annual Large Hadron Collider Physics
13-18 June 2016
Lund, Sweden

[*]Speaker.
[†]on behalf of the CMS and ATLAS collaborations.

© Copyright owned by the author(s) under the terms of the Creative Commons Attribution-NonCommercial-NoDerivatives 4.0 International License (CC BY-NC-ND 4.0).

PoS(LHCP2016)010

1. Introduction

The discovery of the Standard Model (SM) Higgs boson [1, 2] performed by the ATLAS and CMS collaborations [3, 4] has been an important success of the LHC run-1. The measurements of the couplings of the Higgs boson with the other fundamental SM particles may reveal the presence of new physics beyond the SM (BSM). This document presents the combination of the ATLAS and CMS measurements of the Higgs boson production and decay rates and of the Higgs boson coupling with vector bosons and fermions, using approximately $5\,\text{fb}^{-1}$ and $20\,\text{fb}^{-1}$ collected by each experiment of proton-proton collisions at the center-of-mass energy of, respectively, $\sqrt{s} = 7\,\text{TeV}$ and $\sqrt{s} = 8\,\text{TeV}$. A more detailed description of this measurement is reported in [5].

1.1 Assumptions

All measurements presented in this document have been obtained using a few assumptions:

- the Higgs mass is $125.09 \pm 0.21\,(\text{stat.}) \pm 0.11\,(\text{syst.})\,\text{GeV}$ [6];
- the kinematic of the Higgs boson signal is close to the SM prediction (only normalizations are allowed to change);
- Higgs production and decay processes factorize (narrow-width approximation).

1.2 Higgs boson Production channels

The leading SM Higgs boson production processes are:

- gluon-gluon fusion (***gg*F**);
- vector-boson fusion (**VBF**);
- associated production with a vector boson (**VH**):
  - associated production with a W boson (***WH***);
  - associated production with a Z boson (***ZH***);
- associated production with a top quark pair (***ttH***).

The leading-order Feynman diagram of each process is shown in Fig. 1. Additional production channels have been also taken into account since their cross sections can increase largely in case of anomalous Higgs couplings:

- associated production with a single top quark (***tH***);
- associated production with a bottom quark pair (***bbH***).

The cross section of each Higgs production channel and the level of approximation used to evaluate it is shown in Table 1.

PoS(LHCP2016)010

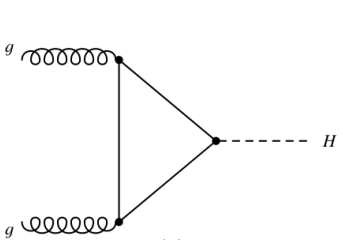

(a) Gluon-gluon fusion.

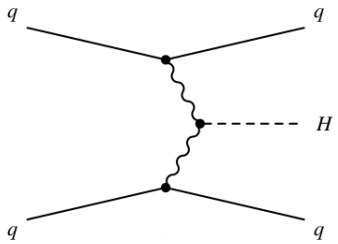

(b) Vector-boson fusion.

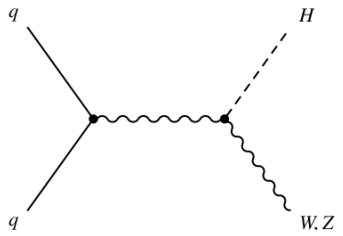

(c) Vector-boson associated production.

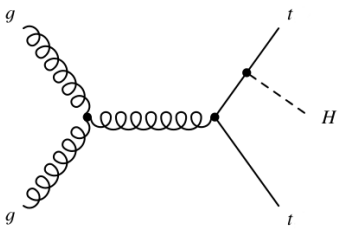

(d) Top-pair associated production.

Figure 1: Leading-order Feynman diagrams of the main Higgs boson production channels.

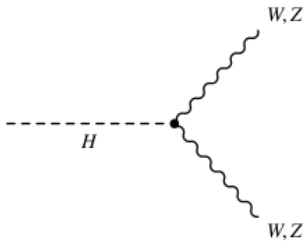

(a) $H \to VV$

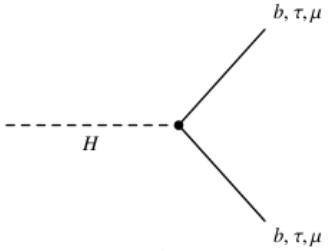

(b) $H \to ff$

Figure 2: Leading-order Feynman diagrams of the Higgs boson decay to massive bosons (left) and fermions (right).

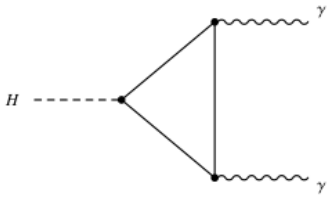

Figure 3: Leading-order Feynman diagrams of Higgs boson decay to $\gamma\gamma$.

PoS(LHCP2016)010

1.3 Higgs boson decay channels

The Higgs boson can decay to massive particles at tree level, as shown in Fig. 2, and to massless particles through loops, as shown in the example of Fig. 3 ($H \to \gamma\gamma$).

Table 2 shows the branching ratio of the SM Higgs boson decay channels for $m_H = 125.09$ GeV. The direct searches for $H \to gg, cc, Zg$ are not included in this combination, but their contributions to the total Higgs width are taken into account.

2. Cross sections and branching ratios fit

2.1 Cross sections times branching ratios fit (23 parameters)

The most generic fit is the measurement of the Higgs boson cross section times branching ratio for each combination of production and decay channel. The measurements are normalized to the SM expectation. Only the five main production (ggF, VBF, WH, ZH, ttH) and decay ($H \to \gamma\gamma, ZZ, WW, \tau\tau, bb$) channels have been taken into account. The $H \to bb$ produced through the VBF and ggF are not included in the fit because the sensitivities of these channels are suppressed by a huge QCD background. The 23 parameters used in the fit are listed in Table 3. Figure 4 shows the best-fitted values obtained combining the ATLAS and CMS results, normalized to the SM expectation. The largest part of the fitted parameters are in within one standard deviation from the SM prediction, the only exceptions are:

- $(\sigma \cdot B)^{WW}_{ttH} : +5.0^{+1.8}_{-1.7}$
- $(\sigma \cdot B)^{WW}_{ZH} : +5.9^{+2.6}_{-2.2}$
- $(\sigma \cdot B)^{bb}_{ZH} : +0.4^{+0.4}_{-0.4}$

Table 1: Standard Model predictions for the Higgs boson production cross sections together with their theoretical uncertainties [7]. The tH cross-section has been taken from [8]. The value of the Higgs boson mass is assumed to be $m_H = 125.09\,\text{GeV}$. The last column shows the level of approximation used to evaluate the Higgs boson cross sections.

Production process	Cross section [pb] $\sqrt{s} = 7$ TeV	Cross section [pb] $\sqrt{s} = 8$ TeV	Order of calculation
ggF	15.0 ± 1.6	19.2 ± 2.0	NNLO(QCD) + NLO(EW)
VBF	1.22 ± 0.03	1.58 ± 0.04	NLO(QCD+EW) + APPROX. NNLO(QCD)
WH	0.577 ± 0.016	0.703 ± 0.018	NNLO(QCD) + NLO(EW)
ZH	0.334 ± 0.013	0.414 ± 0.016	NNLO(QCD) + NLO(EW)
$[ggZH]$	0.023 ± 0.007	0.032 ± 0.010	NLO(QCD)
ttH	0.086 ± 0.009	0.129 ± 0.014	NLO(QCD)
tH	0.012 ± 0.001	0.018 ± 0.001	NLO(QCD)
bbH	0.156 ± 0.021	0.203 ± 0.028	5FS NNLO(QCD) + 4FS NLO(QCD)
Total	17.4 ± 1.6	22.3 ± 2.0	

PoS(LHCP2016)010

- $(\sigma \cdot B)^{\tau\tau}_{WH} : -1.4^{+1.4}_{-1.4}$

2.2 Cross sections and branching ratios fit (9 parameters)

Assuming the existence of only one Higgs boson, the fitted parameter can be factorized in terms of σ^i (cross section) and B^f (branching ratio). In order to cancel out the theoretical uncertainty on the total Higgs cross section, the parameters have been measured with respect to a reference channel ($gg \to H \to ZZ$):

$$\sigma^i \cdot B^f = \sigma(gg \to H \to ZZ) \cdot \left(\frac{\sigma_i}{\sigma_{ggF}}\right) \cdot \left(\frac{B^f}{B^{ZZ}}\right) \tag{2.1}$$

Using this parameterization, the number of free parameters is reduced to nine: one for $gg \to H \to ZZ$, four for the production channel ratios, and four for the decay channel ratios.

Figure 5 shows the nine fitted parameters normalized to the SM. All parameters are compatible with the SM predictions within two standard deviations, with the exception of:

- $\sigma_{ttH}/\sigma_{ggF} : +3.3^{+1.0}_{-0.9}$;
- $B^{BB}/B^{ZZ} : +0.2^{+0.2}_{-0.12}$.

As Figure 6 shows, the likelihood scan of the B^{BB}/B^{ZZ} parameter is asymmetric and its compatibility with the SM is of 2.5 standard deviations. Figure 7 shows that the B^{bb}/B^{ZZ} deficit is anti-correlated with the σ_{ZH}/σ_{ggF} and $\sigma_{ttH}/\sigma_{ggF}$ excesses. The global p-value compatibility between data and SM expectation is 15%.

3. Higgs couplings fit

The σ_i and B^f can be resolved in terms of Higgs boson coupling modifiers κ_i [9]. The parameter $B(WW)$, for instance, depends only on k_W^2.

Table 2: Standard Model predictions for the decay branching fractions of a Higgs boson with a mass of 125.09 GeV, together with their uncertainties [7].

Decay mode	Branching fraction [%]
$H \to bb$	57.5 ± 1.9
$H \to WW$	21.6 ± 0.9
$H \to gg$	8.56 ± 0.86
$H \to \tau\tau$	6.30 ± 0.36
$H \to cc$	2.90 ± 0.35
$H \to ZZ$	2.67 ± 0.11
$H \to \gamma\gamma$	0.228 ± 0.011
$H \to Z\gamma$	0.155 ± 0.014
$H \to \mu\mu$	0.022 ± 0.001

PoS(LHCP2016)010

Table 3: The signal parametrization used to express the $\sigma_i \cdot \mathrm{B}^f$ values for each specific channel $i \to H \to f$. The values labelled with a "$-$" are not measured and are therefore fixed to the SM predictions [5].

Production process	Decay channel				
	$H \to \gamma\gamma$	$H \to ZZ$	$H \to WW$	$H \to \tau\tau$	$H \to bb$
ggF	$(\sigma \cdot \mathrm{B})^{\gamma\gamma}_{gg\mathrm{F}}$	$(\sigma \cdot \mathrm{B})^{ZZ}_{gg\mathrm{F}}$	$(\sigma \cdot \mathrm{B})^{WW}_{gg\mathrm{F}}$	$(\sigma \cdot \mathrm{B})^{\tau\tau}_{gg\mathrm{F}}$	$-$
VBF	$(\sigma \cdot \mathrm{B})^{\gamma\gamma}_{\mathrm{VBF}}$	$(\sigma \cdot \mathrm{B})^{ZZ}_{\mathrm{VBF}}$	$(\sigma \cdot \mathrm{B})^{WW}_{\mathrm{VBF}}$	$(\sigma \cdot \mathrm{B})^{\tau\tau}_{\mathrm{VBF}}$	$-$
WH	$(\sigma \cdot \mathrm{B})^{\gamma\gamma}_{WH}$	$(\sigma \cdot \mathrm{B})^{ZZ}_{WH}$	$(\sigma \cdot \mathrm{B})^{WW}_{WH}$	$(\sigma \cdot \mathrm{B})^{\tau\tau}_{WH}$	$(\sigma \cdot \mathrm{B})^{bb}_{WH}$
ZH	$(\sigma \cdot \mathrm{B})^{\gamma\gamma}_{ZH}$	$(\sigma \cdot \mathrm{B})^{ZZ}_{ZH}$	$(\sigma \cdot \mathrm{B})^{WW}_{ZH}$	$(\sigma \cdot \mathrm{B})^{\tau\tau}_{ZH}$	$(\sigma \cdot \mathrm{B})^{bb}_{ZH}$
ttH	$(\sigma \cdot \mathrm{B})^{\gamma\gamma}_{ttH}$	$(\sigma \cdot \mathrm{B})^{ZZ}_{ttH}$	$(\sigma \cdot \mathrm{B})^{WW}_{ttH}$	$(\sigma \cdot \mathrm{B})^{\tau\tau}_{ttH}$	$(\sigma \cdot \mathrm{B})^{bb}_{ttH}$

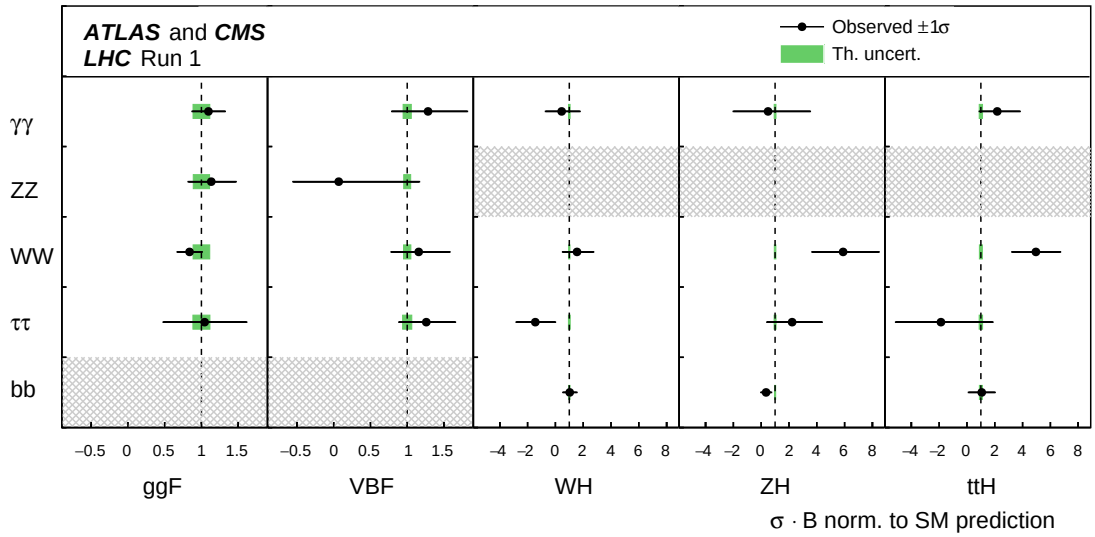

Figure 4: Best fitted cross sections times branching ratios, normalized to the SM prediction (23 parameters fit). The $H \to bb$ produced by ggFand VBF are excluded from the fit because of the large QCD background. The uncertainty on the fitted values for $H \to ZZ$ produced by VH and ttH is very large and so they are not included in the plot [5].

The resolution of σ^i and Γ^f in terms of the coupling modifiers κ_i is shown in Table 4. It specifies also if loops and interference effects are taken into account for each parameter. The effective coupling modifiers κ_γ and κ_g reported in the table are used to search new Physics in the loops of the Higgs-γ and Higgs-gluon interactions, as shown in Fig. 8.

The interference effects are important to determine the relative sign between two couplings. The main interference effects taken into account are the following:

- $\sigma(gg \to H)$: $t - b$ interference (Fig. 9);

PoS(LHCP2016)010

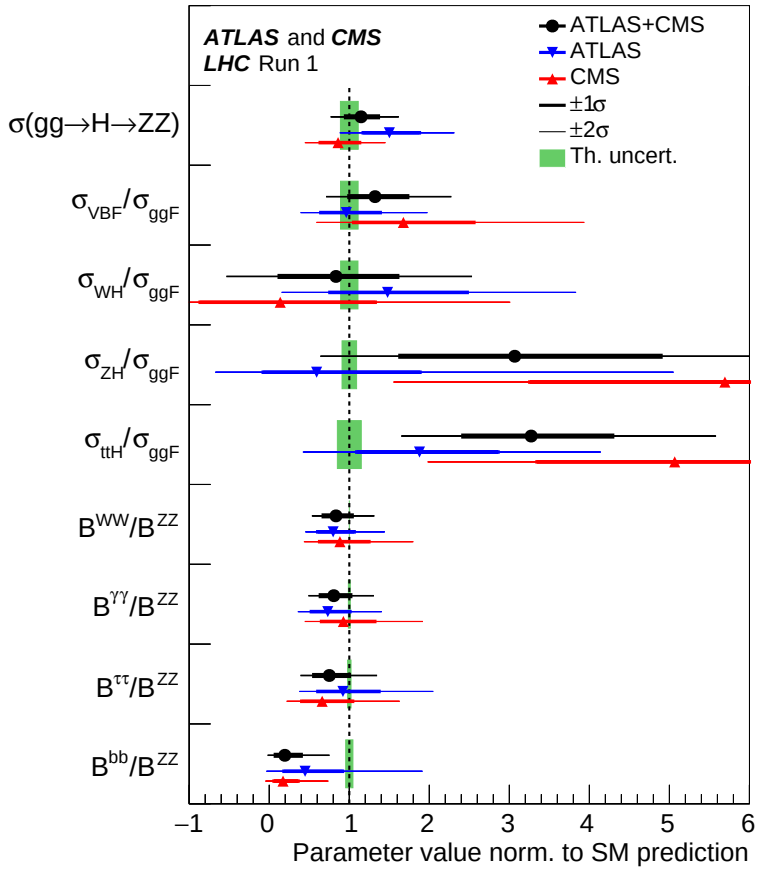

Figure 5: Fit of Higgs cross sections and branching ratios with respect to the $gg \to ZZ$ channel and normalized to the SM prediction (9 parameters fit) [5].

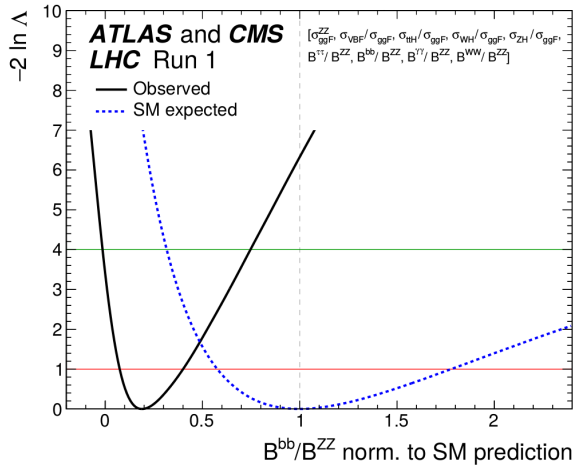

Figure 6: Likelihood scan of BR(bb)/BR(ZZ) normalized to the SM prediction [5].

PoS(LHCP2016)010

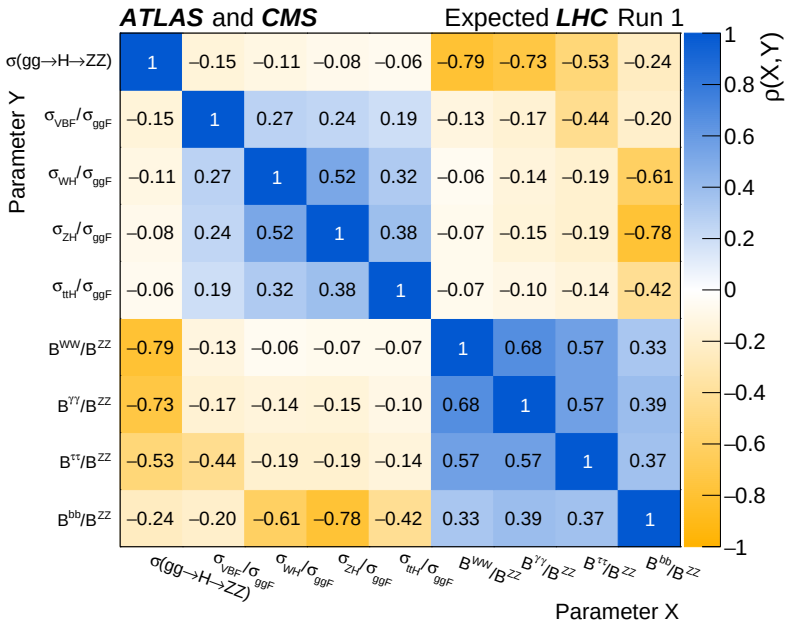

Figure 7: Correlation matrix of the fit reported in Fig. 5 [5].

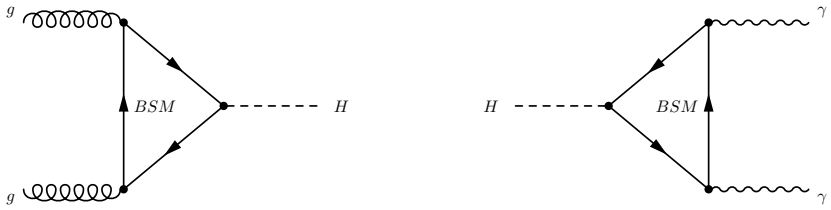

Figure 8: Possible BSM contribution to $gg \to H$ and $H \to \gamma\gamma$.

- $\sigma(gg \to ZH)$: $t - Z$ interference (Fig. 10);
- $\sigma(tHq)$: $t - W$ interference (Fig. 11);
- $\sigma(tHW)$: $t - W$ interference (Fig. 12);
- $B(H \to \gamma\gamma)$: $t - W$ interference (Fig. 13).

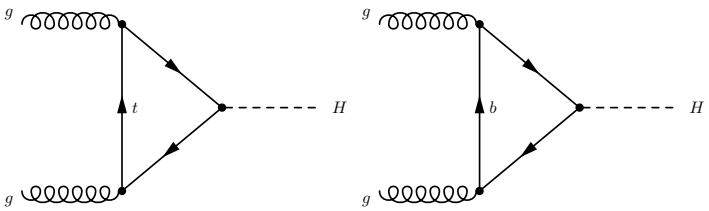

Figure 9: $gg \to H$ ($t - b$ interference).

PoS(LHCP2016)010

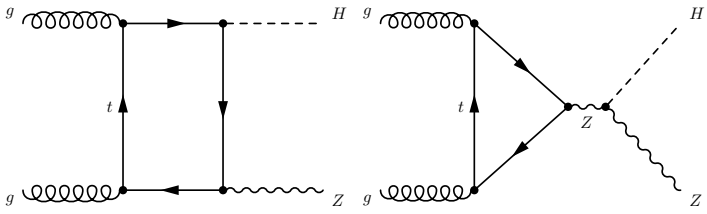

Figure 10: $gg \to ZH$ ($t - Z$ interference).

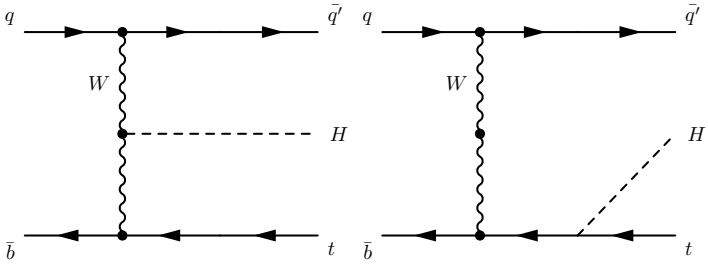

Figure 11: tHq ($t - W$ interference).

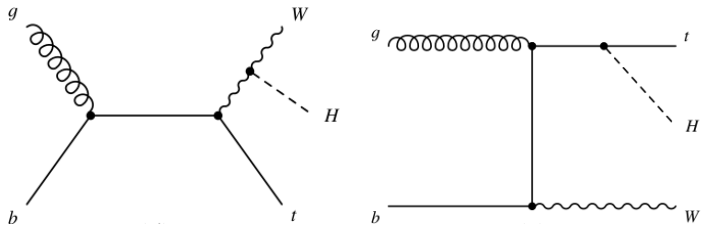

Figure 12: tHW ($t - W$ interference).

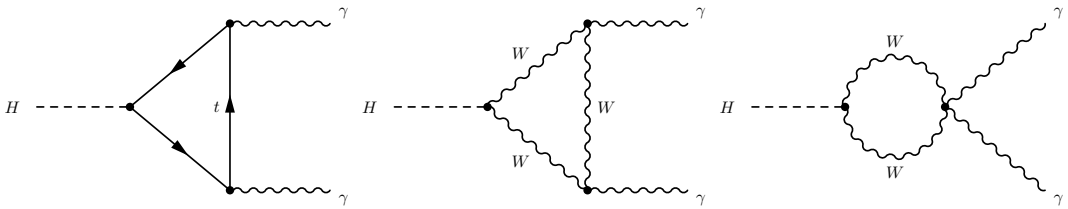

Figure 13: Higgs decay to $\gamma\gamma$ ($t - W$ interference).

3.1 Higgs coupling fit

The fitted Higgs couplings modifiers, using the effective parameter κ_g and κ_γ, are shown in Fig. 14. The fit has been performed both allowing and not allowing BSM Higgs boson decays, defined as:

- decay to weakly interacting stable particles (e.g. dark matter);
- decay to channels that are not directly measured (e.g. $H \to cc$);
- decay with unexpected topology (e.g. $H \to \tau\mu$).

PoS(LHCP2016)010

Indicating with $B_{\rm BSM}$ the total branching ratio of these decay channels, the global Higgs width can be expressed as:

$$\Gamma_H = \frac{k_H^2 \cdot \Gamma_H^{SM}}{1 - B_{\rm BSM}} \tag{3.1}$$

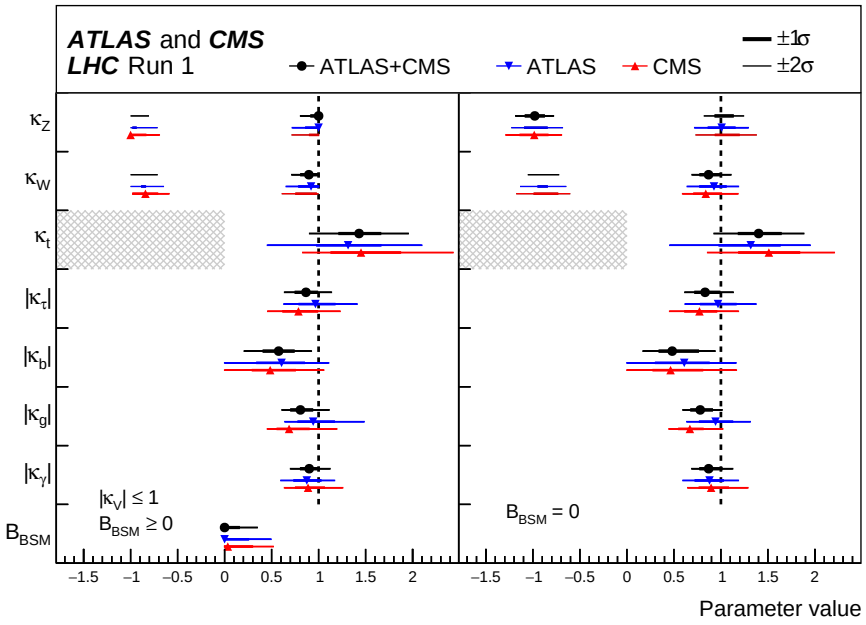

Figure 14: Higgs coupling ratios fit [5]. The κ_t parameter is assumed positive without loss of generality and the hatched area shows the non-allowed region. For those parameters with no sensitivity to the sign, only the absolute values are shown.

The global p-value compatibility with SM of the fit with $B_{\rm BSM} = 0$ is 11%. All κ_i are compatible with the SM within two standard deviations, except for:

$$\kappa_b = 0.49^{+0.27}_{-0.15}. \tag{3.2}$$

The κ_g and κ_γ parameters are in agreement with the SM predictions within two standard deviations:

$$\begin{aligned} \kappa_g &= 0.81^{+0.13}_{-0.10}, \\ \kappa_\gamma &= 0.90^{+0.10}_{-0.09}. \end{aligned} \tag{3.3}$$

The fit with $B_{\rm BSM} \neq 0$ has been constrained to $|\kappa_Z| < 1$ and $|\kappa_W| < 1$ and, as shown in Fig. 14, gives similar results to the previous fit. The 95% CL upper limit of $B_{\rm BSM}$ has been found to be:

- $B_{\rm BSM} < 0.34$ (exp. 0.39);

Figure 15 shows the likelihood scan of the $B_{\rm BSM}$ parameter. This limit may be compared with complementary limits obtained from the direct searches of $H \rightarrow$ invisible:

- ATLAS result: $B_{\rm BSM} < 0.25$ (exp. 0.27) [10];
- CMS result: $B_{\rm BSM} < 0.32$ (exp. 0.26) [11].

PoS(LHCP2016)010

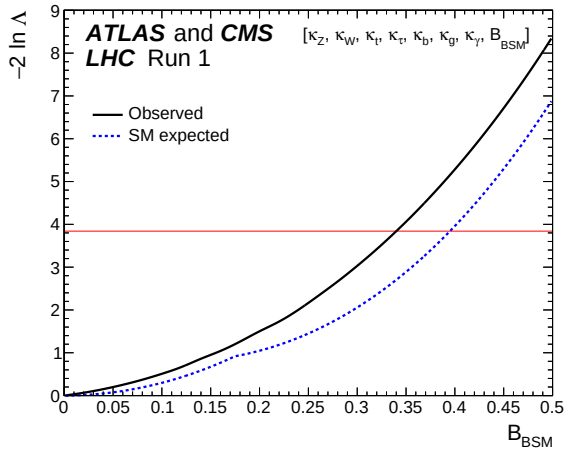

Figure 15: Likelihood scan of B_{BSM} [5].

3.2 Fit of κ_g and κ_γ

As the effective coupling modifiers κ_g and κ_γ are good probes to search for new Physics, a dedicated fit has been performed to measure κ_g and κ_γ constraining all other parameters to the SM predictions. The fit results are compatible with SM and are shown in Fig. 16.

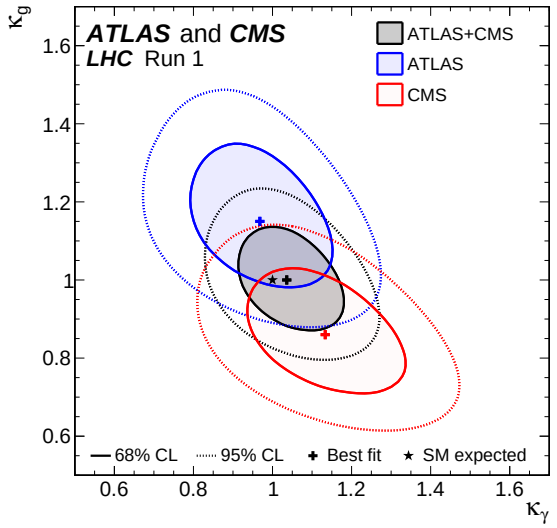

Figure 16: Likelihood scan for κ_g and κ_γ for ATLAS and CMS experiment after the LHC Run 1, and their combination [5].

3.3 Higgs SM-like couplings

Resolving the cross sections and branching fractions with SM (see the last column of Table 4), the fit is still compatible with the SM predictions. The results are shown in Fig. 17: all parameters have been found compatible with SM within two standard deviations and the global p-value compatibility data/SM is 74%.

PoS(LHCP2016)010

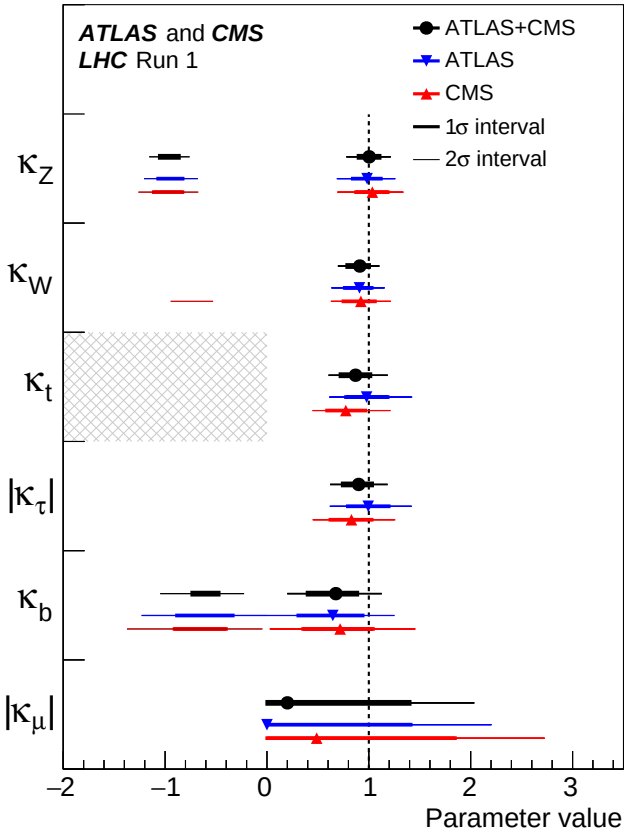

Figure 17: Fitted κ_i values assuming no BSM decay [5]. The κ_t parameter is assumed positive without loss of generality and the hatched area shows the non-allowed region. For those parameters with no sensitivity to the sign, only the absolute values are shown.

3.4 Couplings vs mass

Figure 18 shows the Higgs coupling fit as a function of the particle mass using:

$$\begin{aligned} y &= \kappa_F \frac{m_F}{v} \qquad \text{(for fermions)}, \\ y &= \sqrt{\kappa_V}\frac{m_V}{v} \qquad \text{(for vectors)}. \end{aligned} \tag{3.4}$$

with $v = 245\,\text{GeV}$. The plot has been fitted using a function with two degrees of freedom as suggested in [12]:

$$\begin{aligned} \kappa_{F,i} &= v \cdot m_{F,i}^{\varepsilon}/M^{1+\varepsilon} \qquad \text{(for fermions)}, \\ \kappa_{V,i} &= v \cdot m_{V,i}^{2\varepsilon}/M^{1+2\varepsilon} \qquad \text{(for vectors)}. \end{aligned} \tag{3.5}$$

The results are in good agreement with the SM expectation:

$$\begin{aligned} M &= 233^{+13}_{-12}\,\text{GeV} \qquad (\text{exp.} = 245\,\text{GeV}), \\ \varepsilon &= 0.023^{+0.029}_{-0.027} \qquad (\text{exp.} = 0). \end{aligned} \tag{3.6}$$

PoS(LHCP2016)010

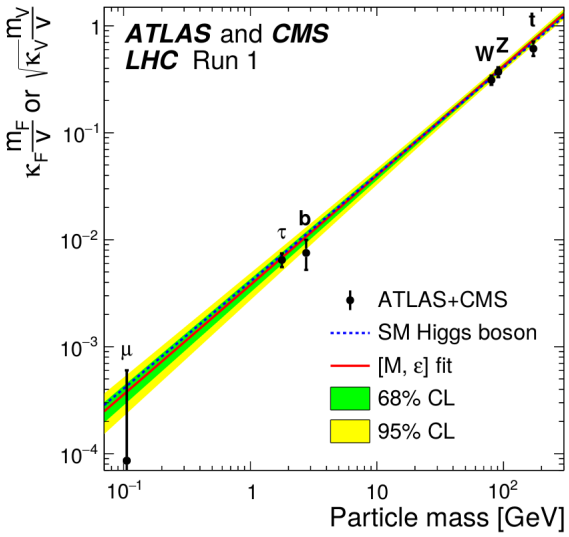

Figure 18: Higgs couplings, as defined in Eq. 3.4, vs particle mass [5]. The plot has been fitted with Eq.3.5 as suggested in [12].

3.5 Vector boson vs fermions

The Higgs couplings have been fitted allowing different couplings in the Higgs production for fermions ($k_F^f = k_t^f = k_b^f = k_t^f = k_\mu^f$) and vectors ($k_V^f = k_Z^f = k_W^f$). The likelihood scan of the two-parameter fit is shown in Fig. 19, for each Higgs decay channel and the combination. Each measurement is compatible with the SM expectation within one standard deviation. In Figure 20, the fit has been repeated using the constraints $k_F^f > 0$ and $k_V^f > 0$. In both cases, the results are compatible with the SM expectations.

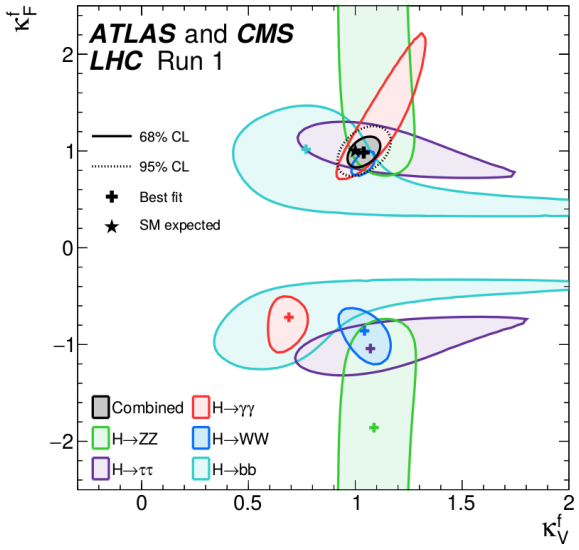

Figure 19: Two-parameter fit of the Higgs couplings in Higgs production for vector bosons (k_V^f) and fermions (k_F^f), for different decay channels and their combination [5].

PoS(LHCP2016)010

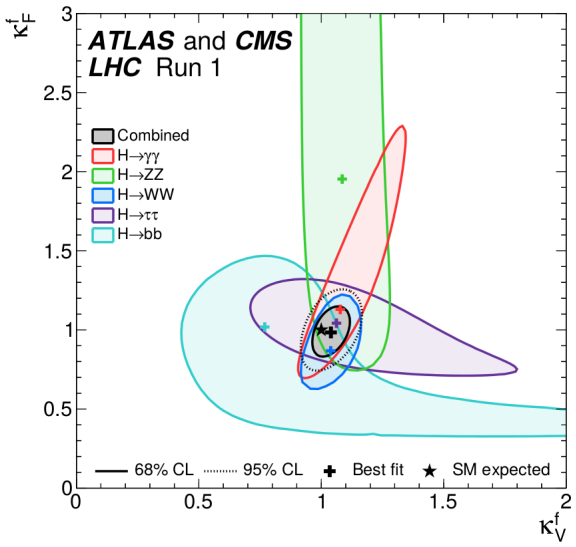

Figure 20: Two-parameter fit of the Higgs couplings in Higgs production for vector bosons (k_V^f) and fermions (k_F^f) in production channel, for different decay channels and their combination. The fit have been constrained to $k_F^f > 0$ and $k_V^f > 0$ [5].

3.6 Higgs coupling ratios

In Sec. 2.2, σ_i and B_f have been fitted with respect to the $gg \to H \to ZZ$ process. Such results can be used to evaluate the ratios of the coupling modifiers with respect to κ_g and κ_Z, as defined in Table 5. As example, $\sigma(ttH)B(bb)/\sigma(gg\mathrm{F})B(ZZ)$ depends on λ_{tg} and λ_{bZ} as follows:

$$\begin{aligned} \sigma_{ttH}B^{bb}/\sigma_{ggF}B^{ZZ} = \\ \kappa_t^2\kappa_b^2/\kappa_q^2\kappa_Z^2 = \\ \lambda_{tg}^2\lambda_{bZ}^2 \end{aligned} \tag{3.7}$$

The result of the coupling modifier ratio fit is shown in Fig. 21. All fitted values are compatible with the SM expectation within two standard deviations, except for:

- $\lambda_{tg} = 1.78^{+0.30}_{-0.27}$;
- $|\lambda_{bZ}| = 0.58^{+0.16}_{-0.20}$.

These two parameters are anti-correlated, as shown in Fig. 22. The global p-value compatibility of the fit with SM is 13%.

3.7 Probing the lepton/quark and up/down-type fermion symmetries

In order to probe the lepton/quark symmetry, we fit data using three free parameters: $\lambda_{lq} = \kappa_{lq}$, $\lambda_{Vq} = \kappa_V/\kappa_q$ and $\kappa_{qq} = \kappa_q \cdot \kappa_q/\kappa_H$. Similarly, it is possible to test the up/down-type fermion symmetries using: $\lambda_{du} = \kappa_{du}$, $\lambda_{Vu} = \kappa_V/\kappa_u$ and $\kappa_{uu} = \kappa_u \cdot \kappa_u/\kappa_H$.

The results of the two fits are shown in Fig. 23. All results are compatible within the SM expectation within one standard deviation.

PoS(LHCP2016)010

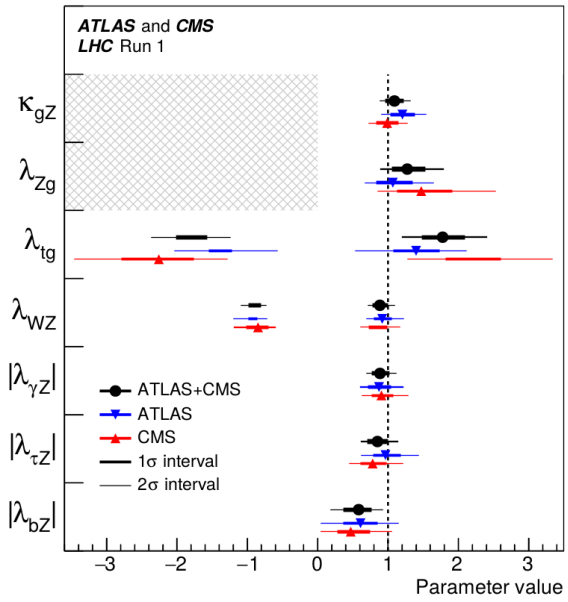

Figure 21: Fitted Higgs coupling ratios [5]. The κ_{gZ} and λ_{Zg} parameters are assumed positive without loss of generality and the hatched areas show the non-allowed regions. For those parameters with no sensitivity to the sign, only the absolute values are shown.

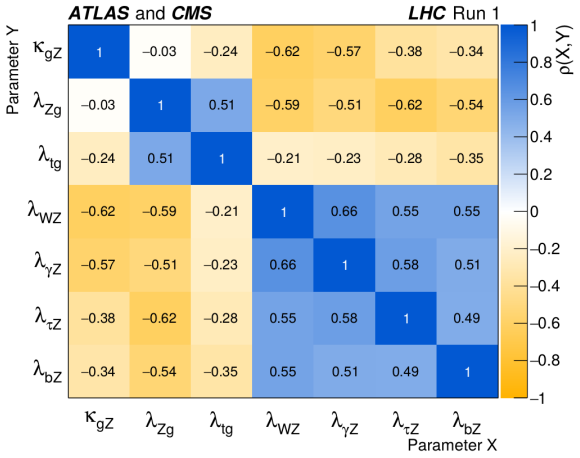

Figure 22: Correlation among the fitted Higgs coupling ratios (Fig. 21) [5].

4. Overall signal strength fit

A one-parameter fit has been performed constraining the branching ratios and cross sections to the SM, but using a global scale factor (signal strength). The fitted signal strength is the following:

$$\mu = 1.09^{+0.11}_{-0.10} = 1.09^{+0.07}_{-0.07}(\text{stat.})^{+0.04}_{-0.04}(\text{exp. syst.})^{+0.03}_{-0.03}(\text{theo. bkg. syst.})^{+0.07}_{-0.06}(\text{theo. sig. syst.}) \quad (4.1)$$

The signal strengths have been also fitted separating the production channels and the decay channels. The results of the two fits are shown in Fig. 24. The p-value of compatibility of data to

PoS(LHCP2016)010

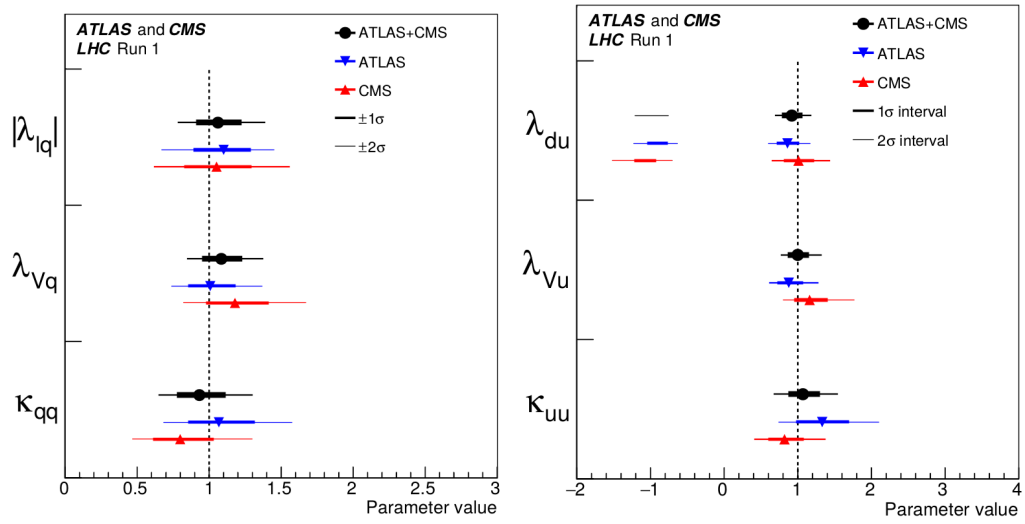

Figure 23: Measurement of Higgs coupling with lepton vs quark (left) and up-quark vs down-quark (right) [5].

SM is of, respectively, 24% and 75%. The only value fitted two standard deviations outside the SM expectation is $\mu_{ttH} = 2.3^{+0.7}_{-0.6}$.

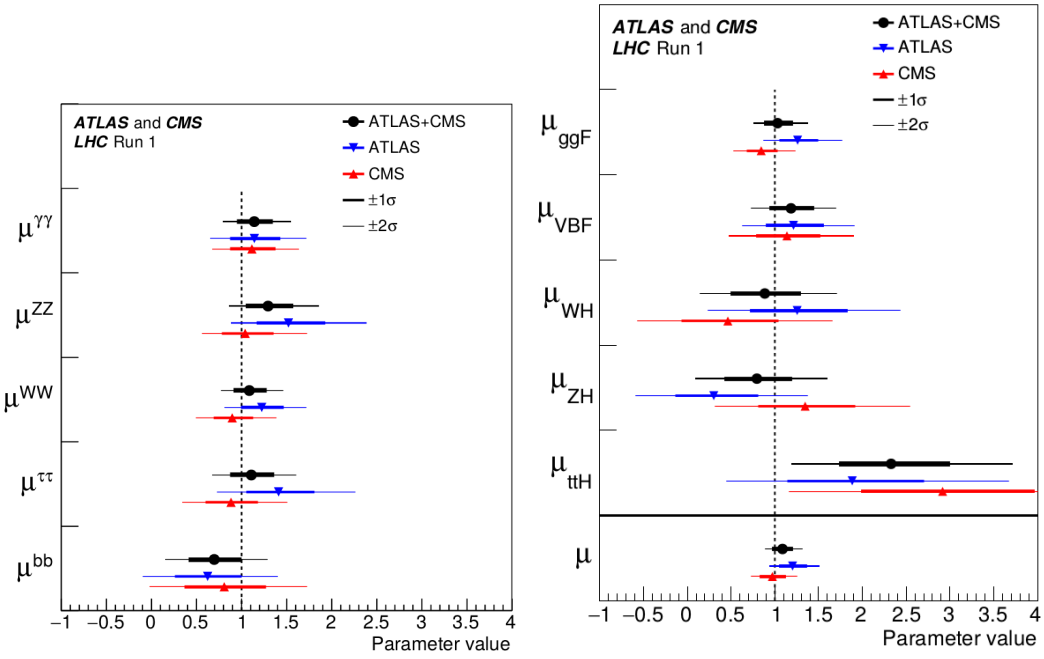

Figure 24: Fitted signal strength for each decay (left) or production (right) channel [5].

These fits can also be interpreted to measure the significance of each Higgs decay and production channel. The results are shown in Tab. 6. Combining ATLAS and CMS data, we observe the vector-boson fusion Higgs production and the $H \to \tau\tau$ decay with more than five standard deviations each.

PoS(LHCP2016)010

4.1 Production asymmetry

To probe possible deviations from SM between the boson and fermion mediated production process, signal strengths have been fitted using six parameters: one for $\mu_{VBF+VH}/\mu_{ggF+ttH}$ and five for the branching ratio of the main production channels. The fitted value for the boson and fermion production asymmetry is $\mu_{VBF+VH}/\mu_{ggF+ttH} = 1.09^{+0.36}_{-0.28}$.

Allowing different $\mu_{VBF+VH}/\mu_{ggF+ttH}$ for each decay channels (ten-parameters fit), the fit is still in good agreement with SM. The results are shown in Fig. 25.

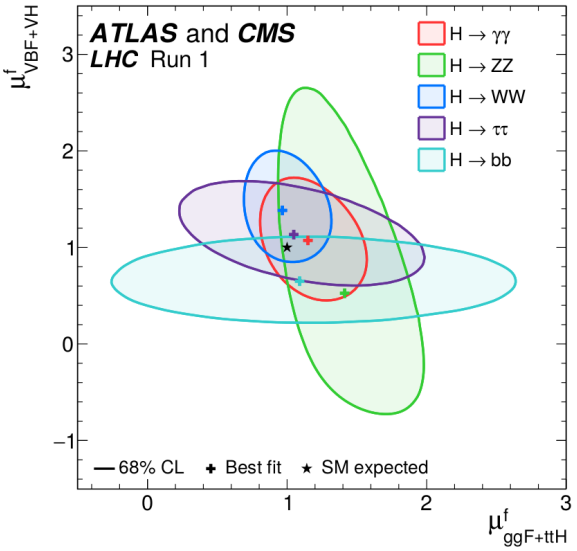

Figure 25: Signal strength boson (μ_{VBF+VH}) and fermion ($\mu_{ggF+ttH}$) mediated production process, considering the five Higgs decay channels [5].

5. Conclusions

A combination of CMS and ATLAS measurements of the Higgs boson production and decay rates have been presented. The couplings to fermions and vector bosons have been measured in different models. No significant deviation from SM has been observed. The global signal strength has been measured 1.09 ± 0.11. Vector-boson fusion and $H \to \tau\tau$ processes have been observed, respectively, with 5.5 and 5.4 standard deviations.

PoS(LHCP2016)010

Table 4: Higgs boson production cross sections σ_i, partial decay widths Γ^f, and total decay width (in the absence of BSM decays) parameterised as a function of the κ coupling modifiers as discussed in the text [5].

Production	Loops	Interference	Effective scaling factor	Resolved scaling factor
$\sigma(gg\mathrm{F})$	✓	t–b	κ_g^2	$1.06\cdot\kappa_t^2+0.01\cdot\kappa_b^2-0.07\cdot\kappa_t\kappa_b$
$\sigma(\mathrm{VBF})$	–	–		$0.74\cdot\kappa_W^2+0.26\cdot\kappa_Z^2$
$\sigma(WH)$	–	–		κ_W^2
$\sigma(qq/qg\to ZH)$	–	–		κ_Z^2
$\sigma(gg\to ZH)$	✓	t–Z		$2.27\cdot\kappa_Z^2+0.37\cdot\kappa_t^2-1.64\cdot\kappa_Z\kappa_t$
$\sigma(ttH)$	–	–		κ_t^2
$\sigma(gb\to tHW)$	–	t–W		$1.84\cdot\kappa_t^2+1.57\cdot\kappa_W^2-2.41\cdot\kappa_t\kappa_W$
$\sigma(qq/qb\to tHq)$	–	t–W		$3.40\cdot\kappa_t^2+3.56\cdot\kappa_W^2-5.96\cdot\kappa_t\kappa_W$
$\sigma(bbH)$	–	–		κ_b^2
Partial decay width				
Γ^{ZZ}	–	–		κ_Z^2
Γ^{WW}	–	–		κ_W^2
$\Gamma^{\gamma\gamma}$	✓	t–W	κ_γ^2	$1.59\cdot\kappa_W^2+0.07\cdot\kappa_t^2-0.66\cdot\kappa_W\kappa_t$
$\Gamma^{\tau\tau}$	–	–		κ_τ^2
Γ^{bb}	–	–		κ_b^2
$\Gamma^{\mu\mu}$	–	–		κ_μ^2
Total width ($\mathrm{B_{BSM}}=0$)				
Γ_H	✓	–	κ_H^2	$0.57\cdot\kappa_b^2+0.22\cdot\kappa_W^2+0.09\cdot\kappa_g^2+$ $0.06\cdot\kappa_\tau^2+0.03\cdot\kappa_Z^2+0.03\cdot\kappa_c^2+$ $0.0023\cdot\kappa_\gamma^2+\ 0.0016\cdot\kappa_{(Z\gamma)}^2+$ $0.0001\cdot\kappa_s^2+0.00022\cdot\kappa_\mu^2$

Table 5: Coupling modifier ratio parameterization using $gg\to H\to ZZ$ channel as a reference [5].

Coupling modifier ratio parameterisation
$\kappa_{gZ}=\kappa_g\cdot\kappa_Z/\kappa_H$
$\lambda_{Zg}=\kappa_Z/\kappa_g$
$\lambda_{tg}=\kappa_t/\kappa_g$
$\lambda_{WZ}=\kappa_W/\kappa_Z$
$\lambda_{\gamma Z}=\kappa_\gamma/\kappa_Z$
$\lambda_{\tau Z}=\kappa_\tau/\kappa_Z$
$\lambda_{bZ}=\kappa_b/\kappa_Z$

PoS(LHCP2016)010

PoS(LHCP2016)010

Table 6: Measured and expected significances for the observation of Higgs boson production processes and decay channels. Not included are the ggF production process and the $H \to ZZ$, $H \to WW$, and $H \to \gamma\gamma$ decay channels, because they have already been clearly observed. All results have been obtained constraining the decay branching fractions to their SM values when considering the production processes, and constraining the production cross sections to their SM values when studying the decays [5].

Production process	Measured significance (σ)	Expected significance (σ)
VBF	5.4	4.6
WH	2.4	2.7
ZH	2.3	2.9
VH	3.5	4.2
ttH	4.4	2.0
Decay channel		
$H \to \tau\tau$	5.5	5.0
$H \to bb$	2.6	3.7

References

[1] Higgs, P. W. , "Broken symmetries, massless particles and gauge fields, *Phys. Lett.* **12**, 132 – 133 (1964).

[2] Englert, F. & Brout, R., "Broken symmetry and the mass of gauge vector mesons" *Phys. Lett.* **13**, 321 – 323 (1964).

[3] The CMS Collaboration, "The CMS experiment at the CERN LHC", *JINST* **3** S08004 (2008).

[4] The ATLAS Collaboration, "The ATLAS Experiment at the CERN Large Hadron Collider", *JINST* **3** (2008) S08003.

[5] CMS and ATLAS collaborations, "Measurements of the Higgs boson production and decay rates and constraints on its couplings from a combined ATLAS and CMS analysis of the LHC pp collision data at $\sqrt{s} = 7$ and 8 TeV.", *JHEP* **08**,045 (2016).

[6] CMS and ATLAS collaborations, "Combined Measurement of the Higgs Boson Mass in pp Collisions at $\sqrt{s} = 7$ and 8 TeV with the ATLAS and CMS Experiments", Phys. Rev. Lett. 114 (2015) 191803

[7] S. Heinemeyer et al., "Handbook of LHC Higgs Cross Sections: 3. Higgs Properties", CERN-2013-004, FERMILAB-CONF-13-667-T

[8] ATLAS Collaboration, Search for $H \to \gamma\gamma$ produced in association with top quarks and constraints on the Yukawa coupling between the top quark and the Higgs boson using data taken at 7 TeV and 8 TeV with the ATLAS detector, *Phys. Lett. B* **740**, 222 (2015).

[9] S. Heinemeyer et al., "Handbook of LHC Higgs Cross Sections: 3. Higgs Properties", CERN-2013-004, FERMILAB-CONF-13-667-T.

[10] ATLAS Collaboration, "Constraints on new phenomena via Higgs boson couplings and invisible decays with the ATLAS detector", *JHEP* **11**,206 (2015)

[11] CMS Collaboration, "Search for invisible decays of a Higgs boson produced via vector boson fusion at $\sqrt{s} = 13$ TeV, CMS-PAS-HIG-16-009

[12] Ellis, John et al. , "Updated Global Analysis of Higgs Couplings" *JHEP* **06**,103 (2013)

PoS(LHCP2016)010